

Influence of atomized powder size on microstructures and mechanical properties of rapidly solidified Al–Cr–Y–Zr aluminum alloys

Yude Xiao · Jue Zhong · Wenxian Li ·
Zhengqing Ma

Received: 13 May 2006 / Accepted: 13 June 2007 / Published online: 10 November 2007
© Springer Science+Business Media, LLC 2007

Abstract Rapidly solidified powders of Al–5.0Cr–4.0Y–1.5Zr (wt%) were prepared by using a multi-stage atomization-rapid solidification powder-making device. The atomized powders were sieved into four shares with various nominal diameter level and were fabricated into hot-extruded bars after cold-isostatically pressing and vacuum degassing process. Influence of atomized powder size on microstructures and mechanical properties of the hot-extruded bars was investigated by optical microscopy, X-ray diffraction, transmission electronic microscopy with EPSPX and scanning electron microscopy. The results show that the fine atomized powders of rapidly solidified Al–5.0Cr–4.0Y–1.5Zr aluminum alloy attains supersaturated solid solution state under the exist condition of multi-stage rapid solidification. With the powder size increasing, there are $\text{Al}_{20}\text{Cr}_2\text{Y}$ (cubic, $a = 1.437$ nm) and $\text{Ll}_2 \text{Al}_3\text{Zr}$ (FCC, $a = 0.407$ nm) phase forming in the powders, and even lumpish particles of $\text{Al}_{20}\text{Cr}_2\text{Y}$ appearing in the coarse atomized powders, as can be found in the as-cast master alloy. Typical microstructures of the extruded bars of rapidly solidified Al–5.0Cr–4.0Y–1.5Zr aluminum alloy can be characterized by fine grain FCC α -Al matrix with ultra-fine spherical particles of $\text{Al}_{20}\text{Cr}_2\text{Y}$ and Al_3Zr . But a small quantity of $\text{Al}_{20}\text{Cr}_2\text{Y}$ coarse lumpish particles with micro-twin structures can be found, originating from lumpish particles of the coarse powders. The extruded bars of rapidly solidified Al–5.0Cr–4.0Y–1.5Zr aluminum alloy

by using the fine powders eliminated out too coarse powders have good tensile properties of $\sigma_{0.2} = 403$ MPa, $\sigma_b = 442$ MPa and $\delta = 9.4\%$ at room temperature, and $\sigma_{0.2} = 153$ MPa, $\sigma_b = 164$ MPa and $\delta = 8.1\%$ at high temperature of 350 °C.

Introduction

For recently three decades rapidly solidified heat-resistant aluminum alloys have been paid a public attention to because of their excellent high-temperature mechanical properties and thermal stability [1–4]. Among them Al–Fe–V–Si, Al–Cr–Zr and Al–Fe–Ce are three most maturely developed alloy systems [5–8]. They become potential candidates substituting for titanium alloy in the temperature range of 150–350 °C, and can be applied in the field of aviation and aerospace industries, to meet with the need of the advanced aircrafts for high-strength heat-resistant lightweight structural materials.

Rapidly solidified Al–Cr–Zr aluminum alloy has its own advantages, in particular having better plastic deforming capability and being easier to produce into various fabricated shapes as compared with Al–Fe–X alloy [5–7]. Main second phases of the Al–Cr–Zr alloy system are equilibrium phase θ - $\text{Al}_{13}\text{Cr}_2$ (monoclinic, $a = 2.52$ nm, $b = 0.76$ nm, $c = 1.10$ nm, $\beta = 109^\circ$) and metastable $\text{Ll}_2\text{Al}_3\text{Zr}$ (FCC, $a = 0.4051$ nm) [8–12]. A lot of past research work focused on improving structural stability of $\text{Ll}_2 \text{Al}_3\text{Zr}$ and suppressing harmful transformation from $\text{Ll}_2 \text{Al}_3\text{Zr}$ into $\text{DO}_{23} \text{Al}_3\text{Zr}$ (Tetragonal, $a = 0.4091$ nm, $b = 1.730$ nm) at elevated temperature by adding of some elements such as Ti, Nb, V, Hf and so on [10–12].

Y. Xiao (✉) · W. Li · Z. Ma
School of Materials Science and Engineering, Central Southern University, Changsha, Hunan 410083, P.R. China
e-mail: xiaoyude@mail.csu.edu.cn

Y. Xiao · J. Zhong
School of Mechanical and Electrical Engineering, Central Southern University, Changsha, Hunan 410083, P.R. China

However, θ -Al₁₃Cr₂ has a large coarsening rate although its crystal structure is very stable. In addition, the monoclinic phase has an unpleasant tendency to developing into lumpish morphology at elevated temperature. Therefore, it is necessary to meliorate crystal structure of the main strengthening phase in the Al–Cr alloy system, which may be of benefit to improving mechanical properties and heat-resistance of rapidly solidified Al–Cr–Zr aluminum alloy.

The references [13–15] pointed out that, main strengthening phase of Al–Cr–Y ternary system was Al₂₀Cr₂Y (cubic, $a = 1.437$ nm), which has an excellent structural stability and a very low ripening rate. Hence, if adding yttrium element into Al–Cr–Zr system, it is possible to develop a new rapidly solidified aluminum alloy with more excellent mechanical properties and heat-resistance. Main objective of this work is to carry out an interesting basic study for further development of the new heat-resistant aluminum alloy.

Experimental procedure

Master alloy with nominal chemical composition of Al–5.0Cr–4.0Y–1.5Zr (mass fraction, %) was prepared by smelting pure Al, and Al–18Cr, Al–10Y, Al–5Zr (mass fraction, %) intermediate alloys in a graphite crucible by using medium frequency induction furnace. The master alloy was remelted and atomized into powders at 930 °C by high pressure nitrogen gas in a multi-stage atomization rapid solidification powder-making device. The atomized powders were sieved by using standard meshes into three shares with various nominal diameter level of L1 ($\bar{D} > 100$ μm), L2 (100 μm $> \bar{D} > 40$ μm), and L3 ($\bar{D} < 40$ μm) powders. The various powders were pressed cold-isostatically into Φ60 mm billets. The billets were manufactured into Φ10 mm in a way of double hot-extrusion at 450 °C after vacuum degassing at 350 °C, and reduction ratios of two-time extrusion were 4/1 (firstly) and 9/1 (secondly).

Size distribution of the atomized powders was analyzed in a SKC-2000 optical sedimenting powder-size meter, and Phase constitution in the various size powder was identified by X-ray diffractometry (XRD) technique, which was carried out in a SIEMENS D500 X-ray diffraction meter with monochromatic Cu-K α radiation (mean wave length being 0.15418 nm) over a 2-theta angle range of 20–90° at a step of 0.02 or 0.03°. Metallographic microstructures were examined in a POLTAR-MET optical microscope. The polished samples were etched in a dilute Keller's reagent of 95% H₂O + 2.5% HNO₃ + 1.5% HCl + 1% HF. The detailed microstructures were characterized by an H800 transmission electronic microscope (TEM). The TEM foils were prepared by twin

jet thinning electrolytically in a solution of 25% nitric acid and 75% methanol (volume fraction) at a temperature of –40 °C and electrical current of 90 mA. An energy disperse X-ray (EPX) detector was used to check composition of second phases in the extruded bars. Tensile properties were measured in an INSTRON 8032 testing machine at room temperature (25 °C) and high temperature (350 °C) at a rate of 0.2 mm/min after soaking for 7 min at testing temperature. A KYKY-AMRAY 2000B scanning electron microscope (SEM) was used to observe fracture surfaces of tensile specimens.

Results and discussion

Apparent characterization and phase identification of the atomized powders

Size distribution of the atomized powders of Al–5.0Cr–4.0Y–1.5Zr alloy and their apparent morphologies are shown in Fig. 1. It indicates that small powders exhibit spherical, and the large powders irregular. A majority of the atomized powders are within the range of 20–100 μm in diameter. X-ray diffraction patterns of the atomized powders are shown in Fig. 2. Aluminum matrix of the L3 ($\bar{D} < 40$ μm) powder attains supersaturated solid solution, in which there is a very little amount of Al₂₀Cr₂Y phase appearing under the exist condition of multi-stage rapid solidification. In the L2 (100 μm $> \bar{D} > 40$ μm), a great amount of Al₂₀Cr₂Y phase is found to form, and a little amount of L1₂ Al₃Zr (FCC, $a = 0.407$ nm) phase also precipitate, which will transform into DO₂₃ Al₃Zr at the temperature higher than 550 °C [12, 15]. In the aluminum matrix of L1 ($\bar{D} > 100$ μm) powder, perhaps more Al₂₀Cr₂Y phase can appear, but θ -Al₁₃Cr₂ is not found.

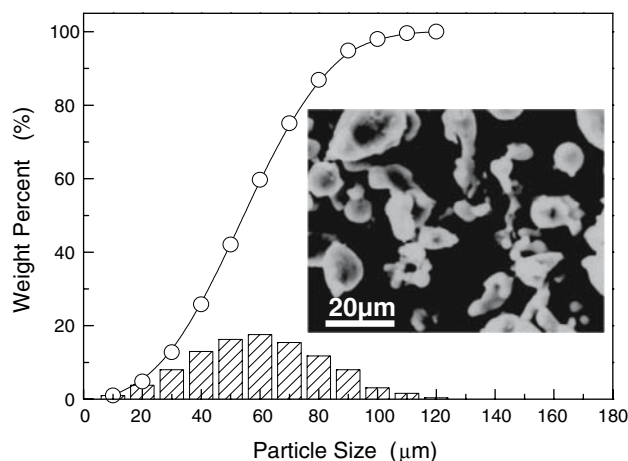


Fig. 1 Size distribution of the atomized powders and their apparent morphologies

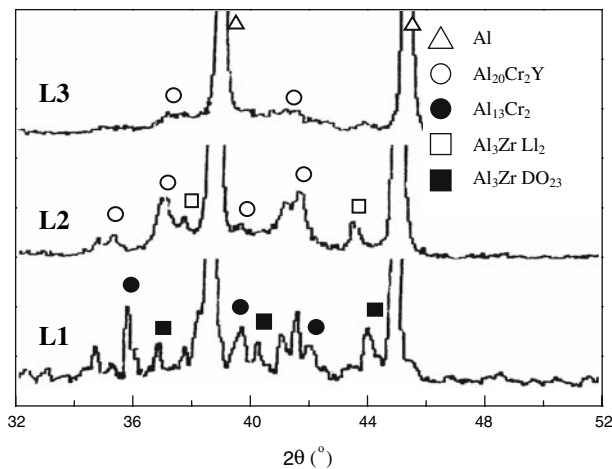


Fig. 2 XRD patterns of the atomized powders of the Al-5.0Cr-3.5Y-1.4Zr alloy

It indicates that, adding yttrium to an Al-Cr-X alloy will impede θ -Al₁₃Cr₂ form, and make the main second phase containing chromium element change from monoclinic Al₁₃Cr₂ into cubic Al₂₀Cr₂Y under the condition of rapid solidification. Therefore, Typical microstructures of the rapidly solidified Al-Cr-Y-Zr powders can be characterized by fine grain FCC α -Al matrix of supersaturated solid solution with two cubic structure second phases, Al₂₀Cr₂Y and L₂ Al₃Zr.

Metallographic characterization of the extruded bars

Metallographic microstructures of the extruded bars prepared by the atomized powders with nominal diameter levels are shown in Fig. 3. The as-extruded microstructures consist mainly of a large amount of ultra-fine intermetallic particles dispersed uniformly in the α -Al matrix. However, as seen in Fig. 3a, in the as-extruded bars of L1 ($\bar{D} > 100 \mu\text{m}$) powders exist lots of inhomogeneous zones with coarse lumpish particles, originating from lumpish particles in the coarse powders as a result of their very

small cooling and solidification rate. After hot extrusion at a large deforming ratio, the atomized powders are compacted into extruded bars with high density approaching 100%. However, seen in Fig. 3c, in the as-extruded bars of L3 ($\bar{D} < 40 \mu\text{m}$) powders some extremely fine powder deformed insufficiently could still be found, and a lot of prior particle boundaries (PPB) between the insufficiently deformed powders are not eliminated completely, as a result of the fact that the fine powders is difficult to deform and their surface oxide film [16, 17] is difficult to be fragmented. Although there are a minor amount of prior particle boundaries that could still be discerned indistinctly, decorated by oxide fragments, in the as-extruded bars of L4 ($\bar{D} < 100 \mu\text{m}$) powders, as well as in those of L2 ($100 \mu\text{m} < \bar{D} < 40 \mu\text{m}$) powders, a majority of the oxide fragments are no longer distinguishable from the intermetallic particles, seen in Fig. 3b and d, after fragmentizing and redistributing under the action of intensive shear deformation during hot extrusion.

Therefore, In the as-extruded bars of rapidly solidified Al-Cr-Y-Zr aluminum alloy the Al₂₀Cr₂Y phase and L₂ Al₃Zr phase exhibit fine spherical particle, but a lot of Al₂₀Cr₂Y lumpish particles can be found in the as-extruded bar of coarse powders, which could be further confirmed via transmission electronic microscopy.

TEM characterization of the extruded bars

Typical TEM microstructures, select area electron diffraction patterns (SAED) and energy disperse X-ray spectrum (EDX) of second phases in the as-extruded bars prepared by the atomized powders with nominal diameter level of L2 ($100 \mu\text{m} > \bar{D} > 40 \mu\text{m}$) are shown in the Fig. 4. There are a large amount of second phase (particles) in grain interior and boundary of the as-extruded bars, seen in Fig. 4a. The SAED and EDX show that the majority of fine particles are identified as Al₂₀Cr₂Y phase, which is cubic structure with lattice parameter of 1.437 nm. The majority of Al₂₀Cr₂Y particles exhibit fine and spherical in the samples prepared by using

Fig. 3 Metallographic microstructures of the extruded bars prepared by the atomized powders with nominal diameter levels (a) L1 ($\bar{D} > 100 \mu\text{m}$), (b) L2 ($100 \mu\text{m} > \bar{D} > 40 \mu\text{m}$), (c) L3 ($\bar{D} < 40 \mu\text{m}$)

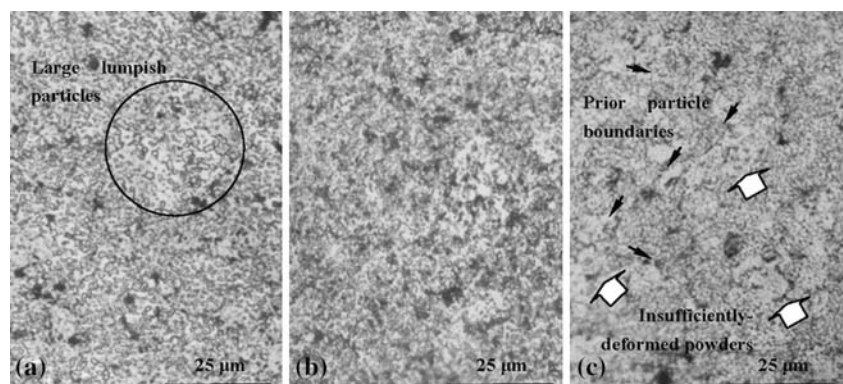
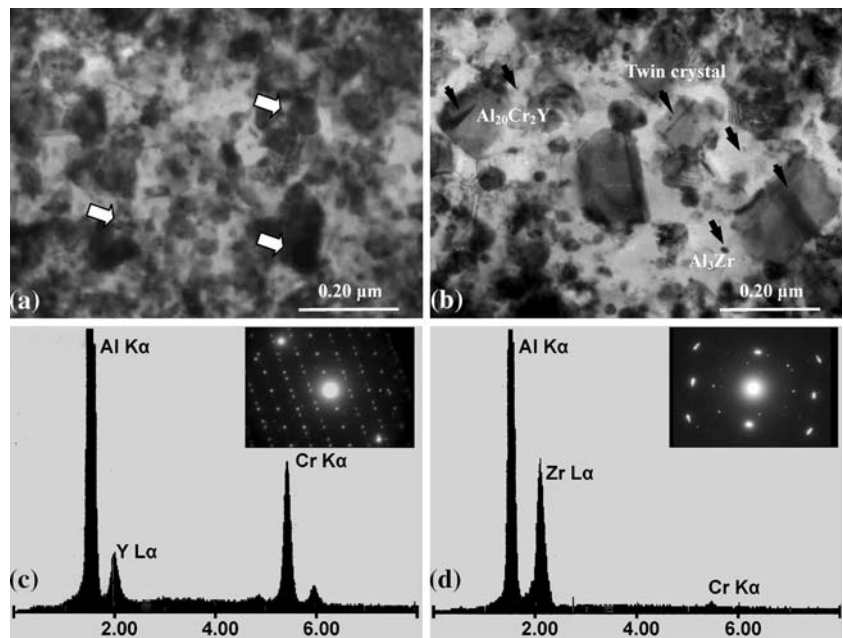


Fig. 4 TEM microstructures of the as-extruded bars prepared by the atomized powders with nominal diameter level of L2 ($100\ \mu\text{m} > \bar{D} > 40\ \mu\text{m}$) (a) Typical TEM microstructures, (b) coarse lumpish particles with twin crystal, (c) SAED and EDX of coarse lumpish $\text{Al}_{20}\text{Cr}_2\text{Y}$, (d) SAED and EDX of fine spherical $\text{L1}_2\ \text{Al}_3\text{Zr}$



the L2 ($100\ \mu\text{m} > \bar{D} > 40\ \mu\text{m}$) powders. However, a few large lumpish $\text{Al}_{20}\text{Cr}_2\text{Y}$ particles of the phase can be found in the samples prepared by using the moderate powders, seen in Fig. 4a and b, and micro-twin structures are found in some of the large lumpish particles, seen in Fig. 4c. In addition, there are some spherical particles with extremely fine size in the $450\ ^\circ\text{C}$ extruded bars of rapidly solidified Al–Cr–Y–Zr aluminum alloys, which was identified as $\text{L1}_2\ \text{Al}_3\text{Zr}$ phase, seen in Fig. 4d. The Al_3Zr phase is able to keep its very ultra-fine dimension and spherical shape due to extremely low diffusion coefficient of zirconium atom in the aluminum matrix.

Typical TEM microstructures and select area electron diffraction patterns (SAED) of $\text{Al}_{20}\text{Cr}_2\text{Y}$ phase in the as-extruded bars prepared by the atomized powders with nominal diameter levels of L1 ($\bar{D} > 100\ \mu\text{m}$) and L3 ($\bar{D} < 40\ \mu\text{m}$) are shown in the Fig. 5. In the samples of L1 coarse powders there are large lumpish $\text{Al}_{20}\text{Cr}_2\text{Y}$ particles or fine spherical particles in a cluster, and in the samples of L3 fine powders the $\text{Al}_{20}\text{Cr}_2\text{Y}$ particles are ultra-fine, which distributed uniformly in the α -Al matrix. The Al_3Zr

phases exhibit ultra-fine and spherical in the as-extruded bars of L1 ($\bar{D} > 100\ \mu\text{m}$) and L3 ($\bar{D} < 40\ \mu\text{m}$) powders.

Mechanical properties and tensile fracture surfaces of the extruded bars

Table 1 gives mechanical properties of the $450\ ^\circ\text{C}$ extruded bars of rapidly solidified Al–5.0Cr–4.0Y–1.5Zr aluminum alloys. The extruded bars by using too coarse powders have lower tensile strength and elongation at room temperature and high temperature ($350\ ^\circ\text{C}$), and the extruded bars by using fine powders have good mechanical properties and thermal stability. However, it is necessary to note that the rapidly solidified Al–5.0Cr–4.0Y–1.5Zr aluminum alloys produced by using too fine powders have very poor elongation at room temperature and high temperature ($350\ ^\circ\text{C}$).

Typical room temperature tensile fracture surfaces of the three extruded bars of the rapidly solidified Al–Cr–Y–Zr alloys are shown in Fig. 6. On the whole, large numbers of dimples distribute uniformly on the fracture surfaces.

Fig. 5 TEM microstructures of the as-extruded bars prepared by the atomized powders with nominal diameter levels (a) L1 ($\bar{D} > 100\ \mu\text{m}$), (b) L3 ($\bar{D} < 40\ \mu\text{m}$)

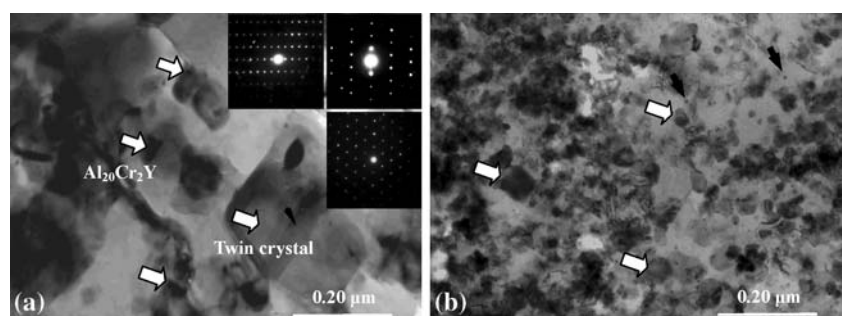
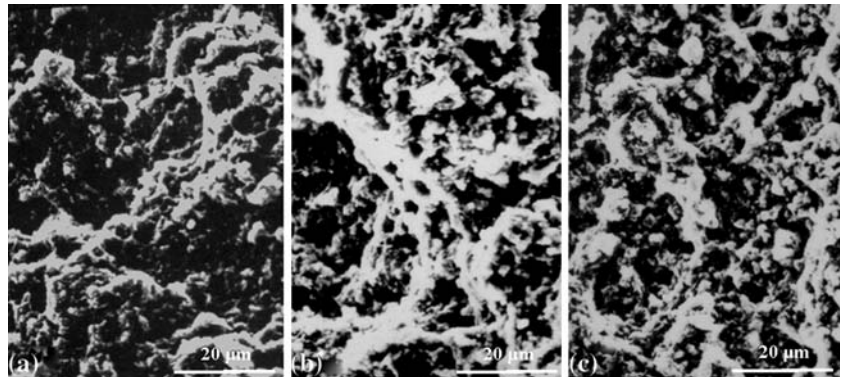


Table 1 Mechanical properties of rapidly solidified Al–5.0Cr–4.0Y–1.5Zr alloys at various temperatures

Level	Size of powders	25 °C			350 °C		
		σ_b (MPa)	$\sigma_{0.2}$ (MPa)	δ (%)	σ_b (MPa)	$\sigma_{0.2}$ (MPa)	δ (%)
L1	$\bar{D} > 100 \mu\text{m}$	392	374	5.4	147	138	4.8
L2	$100 \mu\text{m} > \bar{D} > 40 \mu\text{m}$	442	403	9.4	164	153	8.1
L3	$\bar{D} < 40 \mu\text{m}$	457	418	3.8	178	156	4.3

Fig. 6 Tensile fracture surfaces of three extruded bars of the rapidly solidified Al–Cr–Y–Zr alloys (a) L1, $\bar{D} > 100 \mu\text{m}$, (b) L2, $100 \mu\text{m} > \bar{D} > 40 \mu\text{m}$, (c) L3, $\bar{D} < 40 \mu\text{m}$ 

It indicates that the extruded bars have a good inter-powder binding state, and tensile rupture of the bars carries out in a toughness fracturing mode controlled by growth and coalescence of micro cavities. However, it should be pointed out, on fracture surface of the L1 extruded bars some large dimples with coarse lumpish particles can be found, and fracture surface of the L3 extruded bars is even, with fine and shallow dimples distributed uniformly. Although it also consist of fine dimples, fracture surface of the L2 extruded bars is accidental, with more tearing ridges.

Therefore, the $\text{Al}_{20}\text{Cr}_2\text{Y}$ lumpish particles in the coarse powders and surface oxide film of the fine powders are two factor unbeneficial to improving tensile strength and elongation of the extruded bars rapidly solidified Al–5.0Cr–4.0Y–1.5Zr alloys. Therefore, it is necessary to sieved out too coarse and too fine powders in order to obtain rapidly solidified Al–Cr–Y–Zr alloys with high performances.

Conclusion

(1) The fine atomized powders of rapidly solidified Al–5.0Cr–4.0Y–1.5Zr aluminum alloy attains super-saturated solid solution state under the exist condition of multi-stage rapid solidification. With the powder size increasing, there are $\text{Al}_{20}\text{Cr}_2\text{Y}$ (cubic, $a = 1.437 \text{ nm}$) and $\text{Li}_2 \text{Al}_3\text{Zr}$ (FCC, $a = 0.407 \text{ nm}$) phase forming in the powders, and even lumpish particles of $\text{Al}_{20}\text{Cr}_2\text{Y}$ appearing in the coarse atomized powders.

- (2) Typical microstructures of the extruded bars of rapidly solidified Al–5.0Cr–4.0Y–1.5Zr aluminum alloy can be characterized by fine grain FCC α -Al matrix with ultra-fine spherical particles of $\text{Al}_{20}\text{Cr}_2\text{Y}$ and Al_3Zr . but a small quantity of $\text{Al}_{20}\text{Cr}_2\text{Y}$ coarse lumpish particles with micro-twin structures can be found, originating from lumpish particles of the coarse powders.
- (3) It is necessary to sieved out too coarse and too fine powders to avoid unbeneficial effect of $\text{Al}_{20}\text{Cr}_2\text{Y}$ lumpish particles and surface oxide film on improving tensile strength and elongation. The extruded bars of rapidly solidified Al–5.0Cr–4.0Y–1.5Zr aluminum alloy by using the fine powders have good mechanical properties and thermal stability.

Acknowledgements The authors would like to acknowledge the China Postdoctoral Science Foundation and the Postdoctoral Science Foundation of Central South University for financial support.

References

- Griffith WM, Sanders RE, Hildeman GJ (1982) In: Koczak MJ, Hildeman GJ (eds) High-strength powder metallurgy aluminum alloys. TMS of AIME, TMS Publications, Feb. 17–18, Warrendale, PA, pp 209–218
- Barbaux Y, Pons G (1993) J De Phys 3(7):191
- Xiao Y, Li W, Tan D, Ma Z (2003) Trans Nonfer Soc China 13(3):558
- Bartova B, Vojtech D, Verner J, Gemperle A, Studnicka V (2005) J Alloys Comps 387(1–2):193

5. Skinner DJ (1988) In: Kim Y-W, Griffith WM (eds) Dispersion strengthened aluminum alloys. The Minerals, Metals & Materials Society, TMS-AIME, Warrendale, PA, pp 181–197
6. Marshall GJ, Hughes IR, Miller WS (1986) Mater Sci Technol 2(4):394
7. Lavernia EJ, Ayers JD, Srivatsan TS (1991) Inter Mater Rev 37(1):1–44
8. Silva MP, Jones H, Sellars CM (1991) Mater Sci Eng A134(25):1107
9. Ioannidis EK, Sheppard T (1990) Mater Sci Technol 6(8):749
10. Spencer DN, Brook R, Jones H (1994) Mater Lett 20(3–4):125
11. Octor H, Naka S (1989) Philos Magaz Lett 59(5):229
12. Chuang MS, Tu GC (1994) Script Metal et Mater 31(9):1259
13. Hawk JA, Angers LM, Wilsdorf HGF (1988) In: Kim Y-W, Griffith WM (eds) Dispersion strengthened aluminum alloys. The Minerals, Metals & Materials Society, TMS-AIME, Warrendale, PA, pp 339–346
14. You B-S, Park W-W (1996) Script Mater 34(2):201
15. Xiao Y-D, Li W-X, Li W, Li S-R, Ma Z-Q (2002) Trans Nonfer Metals Soc China 12(1):16
16. Carney TJ, Tsakiroopoulos P, Watts JF, Castle JE (1990) Int J Rapid Solid 5(2–3):189
17. Yamasaki M, Kawamura Y (2004) Mater Trans 45(4):1335